OPEN ACCESS Freely available online

Journal of Proteomics & Bioinformatics

Research Article

Physiological and Proteomic Analysis of *Brassica napus* in Response to Salt Stress

Bing Yu[1,2,3], Gang Chen[3,4], Huizi DuanMu[1,2], Daniel Dufresne[3,5], John E. Erickson[6,7], Jin Koh[3], Haiying Li[1,2*], Sixue Chen[3,7,8*]

[1]Engineering Research Center of Agricultural Microbiology Technology, Ministry of Education, Heilongjiang University, Harbin 150500, China; [2]College of Life Science, Heilongjiang University, Harbin 150080, China; [3]Department of Biology, Genetics Institute, University of Florida, Gainesville, FL 32610, USA; [4]Yangzhou University, Yangzhou, 225009 Jiangsu, China; [5]Department of Chemistry, Florida Atlantic University, Boca Raton, FL 33431, USA; [6]Agronomy Department, University of Florida, Gainesville, FL 32611, USA; [7]Plant Molecular and Cellular Biology Program, University of Florida, Gainesville, FL 32610, USA; [8]Proteomics and Mass Spectrometry, Interdisciplinary Center for Biotechnology Research (ICBR), University of Florida, Gainesville, FL 32610, USA

ABSTRACT

Salinity is a major abiotic stress that adversely affects plant growth and development. Canola (*Brassica napus L.*) is an important oilseed crop in the world, and its yield decreases drastically with increasing salinity. To date, little is known about the molecular mechanisms underlying its salt stress response and tolerance. This study combines physiological assays with comparative proteomics to understand how *B. napus* plants respond to salt stress. The changes in relative water content, electrical conductance, stomata conductance, intercellular CO_2 concentration, transpiration rate, photosynthesis rate, water usage efficiency, respiration rate, chlorophyll fluorescence, antioxidant enzyme activities, soluble sugar, proline and betaine in *B. napus* plants under different NaCl concentrations were analyzed. Proteomic profiles of *B. napus* plants under 100, 200 and 400 mM NaCl treatment at 7 day and 14 day were acquired using iTRAQ LC-MS/MS based quantitative proteomics. A total of 2316 proteins were identified in *B. napus* leaves, of which 614 proteins showed differential expression under salt stress. These proteins were mainly involved in 10 processes, of which proteins in stress and defense, metabolism and photosynthesis pathways ranked the top three. Subcellular localization analysis showed that most proteins were located in chloroplast, cytoplasm, mitochondria and nucleus. A total of 138 differentially expressed proteins were predicted to interact with each other. These results have provided a comprehensive view of the physiological and molecular processes taken place in *B. napus* leaves under salt stress, and revealed the molecular mechanisms underlying salt tolerance of *B. napus* plants.

Keywords: *Brassica napus*; Salt stress; Physiological analysis; Proteomics; iTRAQ LC-MS/MS

ABBREVATIONS

APX: Ascorbate Peroxidase; AsA-GSH cycle: Ascorbate-glutathione Cycle; ATPS: ATP Sulfurylases; CA: Carbonic Anhydrase; CAB: Chlorophyll a b-binding Protein; CAT: Catalase; Ci: Intercellular CO_2 Concentration; Cond: Stomatal Conductance; CS: Cysteine Synthases; CYP: Chaperone/Chaperonin Proteins; Cytb6f: Cytochrome b6-f Complex Protein; DEPs: Differentially Expressed Proteins; 2-DE: Two-dimensional Gel Electrophoresis; DW: Dry Weight; ER: Endoplasmic Reticulum; FNR: Ferredoxin NADP+ Reductase; FW: Fresh Weight; GADPH: Glyceraldehyde-3-phosphate Dehydrogenase; Gly I: Glyoxalase I; Gly II: Glyoxalase II; GO: Glycolate Oxidase; GPX: Guaiacol Peroxidase; GR: Glutathione Reductase; GSH: Reduced Glutathion; GS: Glutamine Synthetase; GST: Glutathione S-Transferase; HK: Histidine Kinases; HSPs: Heat Shock Proteins; iTRAQ: Isobaric Tagging for Relative and Absolute Quantification; MG: Methylglyoxal; NO: Nitric Oxide; OEE2: Oxygen-Evolving Enhancer Protein 2; OEC: Oxygen-Evolving Complex; PDI: Protein Disulfide-Isomerase; PGK: Phosphoglycerate Kinase; PKS5: PROTEIN KINASE5; PMA: Plasma Membrane ATPase; Pn: Photosynthesis Rate; POD: Peroxidase; POR: Protochlorophyllide Reductase; PPase: Pyrophosphatase; PPIase: Peptidyl-prolyl cis-trans Isomerase; PPIs: Protein-protein Interactions; PRK: Phosphoribulokinase Precursor; PrxR-Trx cycle: Peroxiredoxin-thioredoxin pathway; RCA: RubisCO Activase; REC: Relative Electrical Conductance; ROS: Reactive Oxygen Species; RPI: Ribulose-5-phosphate Isomerase; RR: Two-component System Response and Regulator;

Correspondence to: Haiying Li, College of Life Science, Heilongjiang University, Harbin, China, Tel: + 0451-86609753; E-mail: lvzh3000@sina.com

Sixue Chen, Department of Biology, Genetics Institute, University of Florida, Gainesville, USA, Tel: +352-273-8057; E-mail: schen@ufl.edu

Received: January 26, 2021, **Accepted:** February 09, 2021, **Published:** February 16, 2021

Citation: Yu B, Chen G, DuanMu H, Dufresne D, Erickson JE, Koh J, et al. (2021) Physiological and Proteomic Analysis of *Brassica napus* in Response to Salt Stress. J Proteomics Bioinform. 14:523.

RubisCO: Ribulose 1,5-biphosphate Carboxylase/Oxygenase; RWC: Relative Water Content; S: Sulfur; Se: Selenite; SLG: S-lactoylglutathione; SOD: Superoxide Dismutase; SOS: Salt-Overly-Sensitive; TK: Transketolase; TPI: Triosephosphate Isomerase; Tr: Transpiration Rate; VHA: V-type H+-ATPase; WUE: Water-Use Efficiency

INTRODUCTION

Plants are constantly challenged by various biotic and abiotic stresses during their life cycle, which negatively affect their growth, development and productivity [1,2]. Salinity as one of the major abiotic stresses affects more than 800 million hectares of land, equivalent to more than 6% of the earth area [3-5]. Approximately 400 million hectares of agricultural land are affected by salinity and this number keeps going up [6]. Therefore, salt stress poses a major global problem for agriculture. It has stimulated immense interest in elucidating salt tolerance mechanisms and developing strategies toward boosting crop salt tolerance [7,8].

Salt stress causes perturbation to many plants physiological and biochemical processes, including photosynthesis, nutrient and water uptake, root growth, and cellular metabolism [9-11]. Plant responses to salt stress include the following phases [1]: Salinity causes low water potential of roots, resulting in osmotic stress. Meanwhile, Na^+ and Cl^- ions are transported to the shoots, resulting in ionic stress. Subsequently, increased production of reactive oxygen species (ROS) leads to oxidative stress. The osmotic stress, ionic toxicity and oxidative stress cause deleterious effects to plants [12,13]. To survive salt stress, plants respond and adapt with sophisticated mechanisms that include developmental, morphological, physiological and biochemical strategies and require alterations in gene expression and changes in the protein profiles [7,14,15]. At physiological level, plants have developed cellular adjustment strategies to reduce salt stress damages, e.g., accumulating compatible solutes (soluble sugars, proline and betaine) [15,16], excluding Na^+ and Cl^- in roots [5] and scavenging of ROS [17]. The effectiveness of the plant antioxidant system can be measured by the activities of the ROS-scavenging enzymes such as superoxide dismutase (SOD), ascorbate peroxidase (APX), catalase (CAT), glutathione reductase (GR), guaiacol peroxidase (GPX) and peroxidase (POD) [18-21].

Many salt stress responsive genes in different plants have been identified [22,23]. For example, 1696 genes in rice (*Oryza sativa*) [24], 2696 genes from Soybean (*Glycine max*) [25], 7217 genes from *Arabidopsis thaliana* [26], 472 genes from maize (*Zea mays*) [27], 163 genes from Canola (*B. napus*) [28], 3310 genes from two genotypes of *Medicago truncatula* [29], and 840 genes from wheat (*T. aestivum* cv. Chinese Spring) [30] showed differential expression under salt stress. However, transcriptomic approaches may only partially contribute to the understanding of plant stress responses because many transcripts may undergo a number of posttranscriptional modifications, and even do not make proteins [7,31]. Proteomics, the large-scale study of proteins, has the potential to fill this gap. Proteins are "actor" molecules and a profound analysis of the proteome is essential to understanding the molecular mechanisms underlying plant salt stress response [1]. Recently, isobaric tagging for relative and absolute quantification (iTRAQ)-based quantitative proteomics approach [32,33] was used to identify salt responsive proteins in several plant species [14,34-40]. For example, 31 and 32 differentially expressed proteins (DEPs) in leaves of *A. thaliana* and *Thellungiella halophila* under salt stress were identified, respectively [14]. In rice shoots, 56 DEPs were identified after salt stress treatment [34], and in rice suspension cells 521 salt stress responsive proteins were identified [35]. In maize roots, 28 salt-responsive proteins were identified [36]. In tomato roots, 313 proteins responsive to NaCl and $NaHCO_3$ were observed [37]. In sugar beet leaves and roots, 75 and 43 DEPs under salt stress were identified, respectively [38]. In the chloroplasts of *Kandelia cande* [39] and in the leaves of *Tangut Nitraria* [40], 76 and 71 DEPs were identified, respectively.

Canola (*Brassica napus* L.) belongs to the family of Brassicaceae. Canola is the third most important oilseed crop after palm and soybean, cultivated worldwide for oil production [41]. Canola oil, rich in polyunsaturated fatty acids, is considered a healthy ingredient. Canola is also considered as one of the essential sources for biodiesel fuel [42,43]. Like other important crops, environmental stresses reduce canola yield and production. Although physiological changes in Canola under salt stress have been studied [44-49], the studies did not include comprehensive physiological analyses to include relative water content, electrical conductance, photosynthesis, chlorophyll fluorescence, soluble sugar, proline, betaine contents and antioxidant enzyme activities at different time points under different levels of salt stress. To date, only a few proteomic studies in Canola under salt stress have been reported. Bandehagh *et al.* identified 46 proteins in canola leaves under salt stress (0, 175 mM and 350 mM NaCl) at one time point using 2-DE (two-dimensional gel electrophoresis) approach [50]. The single time point snapshot missed dynamic protein changes in the course of plant response to salt stress. Other 2-DE proteomics of canola salt stress responses only identified 42 [51] and 21 proteins [52]. It is well-known that the 2D gel approach is limited to mostly abundant proteins [53-55]. A recent gel-free proteomics on how *Pseudomonas fluorescens* bacteria improved canola tolerance to salt stress identified a couple of hundred proteins [56]. In addition, proteomic changes of canola under drought stress over a 14-day period were examined using iTRAQ LC-MS/MS. A total of 1976 proteins expressed during drought were identified, revealing changes of protein abundance and post-translational modifications (PTMs) [57].

In the present work, physiological and proteomic changes of *B. napus* in response to different levels of salt stress were profiled in a time course study. Different types of morphological and physiological data were obtained from *B. napus* seedlings treated with 0, 50 mM, 100 mM, 200 mM and 400 mM NaCl for different periods of time. Then an iTRAQ-based quantitative proteomics approach was used to identify and quantify DEPs in the leaves under 100 mM, 200 mM and 400 mM NaCl treatments for 7 days and 14 days, respectively. This is a large-scale study using iTRAQ 2D LC-MS/MS in profiling proteomic

changes in leaves of canola plants under salt stress. The results have enhanced understanding of *B. napus* salt-responsive proteins and their potential functions, and provided a comprehensive view of the physiological and molecular processes in the leaves under salt stress, which lead to deeper insights into the molecular mechanisms underlying canola salt stress tolerance.

MATERIALS AND METHODS

Plant material and salt treatments

Seeds of the *B. napus* var. Global were germinated in a Metro-Mix 500 potting mixture (The Scotts Co., Marysville, OH, USA), and plants were grown in a growth chamber under a photosynthetic flux of 160 µmol of photons m^{-2} s^{-1} with a photoperiod of 10 h at 24°C in light and 12 h at 20°C in dark. When the seedlings reached four-week old, they were transplanted into pots filled with perlite and vermiculite (1:1), and watered with a half-strength Hoagland solution. Two weeks later, the seedlings were treated with 0, 50 mM, 100 mM, 200 mM and 400 mM NaCl with the salt concentration increased in aliquots of 100 mM every day until the 200 mM and 400 mM were reached. On day 3, 5, 7, 10, 12 and 14 after treatment, the third full expanded leaf from the top was selected for physiological assays or immediately frozen in liquid nitrogen and stored at -80°C for proteomics experiments. Three independent biological replicates for each control or treatment were conducted for all the experiments.

Physiological analyses of control and salt-stressed plants

Relative water content (RWC) of leaves: After different periods of salt treatment, fresh weight (FW) was measured immediately after the leaves were harvested. Dry Weight (DW) was obtained after drying the samples at 75°C for 48 hours. Turgor weight was determined by subjecting the leaves to rehydration for two hours after their fresh weight was determined. For each experiment, RWC was determined according to a previous method [58]: RWC(%)=(FW-DW) / (turgor weight-DW) × 100.

Relative Electrical Conductance (REC) of leaves: The REC of leaves was measured as described by Dionisio-Sese and Tobita 1998 [59], using a Fisher Scientific Accumet Excel XL30 conductivity meter. The REC was expressed as EL(%) = $(EC_1-EC_0) / (EC_2-EC_0)$ × 100. EC_1 represents the initial electrical conductivity of the medium, and EC_2 indicates the final electrical conductivity of the medium after being autoclaved at 121°C for 20 min, while EC_0 shows the electrical conductivity of distilled water.

Photosynthesis and chlorophyll fluorescence analysis: Gas exchange measurements, such as stomatal conductance (Cond), intercellular CO_2 concentration (Ci), transpiration rate (Tr), and photosynthesis rate (Pn), were determined at 10:00 am with a LI-6400XT photosynthesis system (LI-COR Inc., Lincoln, NE, USA), and the respiration rate was determined at 10:00 pm in dark. Water-use efficiency (WUE) was calculated from Pn divided by Tr [8]. The chlorophyll fluorescence parameters (Fv/Fm and Fv/Fo) was measured using a Handy PEA portable fluorescence spectrometer (Hansatech Instruments, Ltd., King's Lynn, UK) [60].

Antioxidant enzyme activity assay: Leaves of 0.5 g FW were homogenized in 100 mM potassium phosphate buffer (pH 7.8) containing 0.1 mM EDTA, 1 % (w/v) PVP, 0.5 % (v/v) Triton X-100, 5 mM ascorbate. The homogenate was centrifuged at 10 000 g for 20 min at 4°C. The supernatant was collected for measurements of antioxidant enzyme activities: 1) Superoxide dismutase (SOD) activity was determined as described by Stewart and Bewley [61]. The reaction mixture (3 ml) consisted of 50 mM phosphate buffer (pH 7.8), 13 mM methionine, 75 mM nitroblue tetrazolium, 100 mM EDTA and 2 mM riboflavin. After adding 0.1 ml of enzyme extract, test tubes were shaken and placed 30 cm below a light source (30 W fluorescent lamps). The reaction was started by switching-on the light. The reaction was allowed for 30 min and then stopped by switching-off the light. The tubes were kept in the dark until absorbance reading. The reaction mixture, which was not exposed to light did not develop color and served as control. The absorbance was measured at 560 nm in a spectrophotometer. Log A560 was plotted as a function of the volume of enzyme extract used in the reaction mixture. The volume of the enzyme extract corresponding to 50% inhibition of the reaction was read and considered as one enzyme unit and expressed as unit mg^{-1} protein. 2) Ascorbate peroxidase (APX) activity was determined in 3 ml of reaction mixture containing 50 mM potassium phosphate (pH 7.0), 0.5 mM ascorbate (extinction coefficient ε=2.8 mM cm^{-1}), 0.1 mM EDTA, 1.5 mM H_2O_2 and 0.1 ml of the enzyme extract. The linear decrease in absorbance at the wavelength of 290 nm was followed for 1 min as described by Nakano and Asada [62]. The reaction was initiated by addition of H_2O_2. The activity of APX was calculated in terms of µmol ascorbic acid oxidized min^{-1} mg^{-1} protein. 3) Glutathione S-Transferase (GST) activity was measured at 25°C in a reaction mixture of 3 ml (1.5 ml 50 mM pH 7.0 phosphatic buffer, 0.3 ml 1 mM GSH, 0.3 ml 1mM 1-chloro-2,4-dinitrobenzene (CDNB), and 0.1 ml enzyme extract, and the reaction mixture without CDNB was used as control. The enzyme activity was calculated based on the change of absorbance at 340 nm in 1 min [63]. 4) Catalase (CAT) activity was determined by a modification of the spectrophotometric method [64]. The reaction mixture contained 50 mM phosphatic buffer (pH 7.0), 20 mM H_2O_2 and 0.1 ml enzyme extract. The reaction was initiated by addition of H_2O_2. The change in absorbance at 240 nm was monitored for 3 min. The enzyme activity was calculated based on the change of absorbance at 240 nm in 3 min (OD240 • min^{-1} • mg^{-1} protein).

Biochemical analysis of control and salt stressed plants

Analysis of soluble sugar, proline and betaine content: After sampling, fresh leaves were lyophilized and ground into fine powder for proline and sugar analysis. Total soluble sugar and proline contents were determined using ninhydrin reaction and an anthrone reagent, respectively [65]. Betaine content was determined with fresh leaves using Reinecke salt as previously described [66].

Statistical analysis of physiological and biochemical data: To

determine whether there are significant differences in the data across different time points of salt stress treatment, analysis of variance (ANOVA) was performed using JMP 10.0.2 (SAS Institute, Cary, NC, USA). A two-sample t-test was performed to assess whether control and salt-stressed samples differ significantly at each time point.

Protein extraction, digestion, iTRAQ labeling and LC-MS/MS

Proteins were extracted and quantified as previously described [67], and dissolved in 0.1% SDS, 0.5 M triethylammonium bicarbonate, pH 8.5. For each sample, a total of 100 μg of protein were reduced, alkylated, trypsin-digested, and labeled according to the manufacturer's instructions (AB Sciex Inc., Foster City, CA, USA). The control, 100 mM, 200 mM and 400 mM NaCl treated samples at 7 day were labeled with iTRAQ tags 113, 114, 115 and 116, and the corresponding 14 day samples were labeled with iTRAQ tags 117, 118, 119 and 121, respectively. Two independent experiments were carried out with different biological samples. Labeled peptides were desalted with C18-solid phase extraction and dissolved in strong cation exchange (SCX) solvent A (25% (v/v) acetonitrile, 10 mM ammonium formate, and 0.1% (v/v) formic acid, pH 2.8). The peptides were fractionated using an Agilent HPLC 1260 with a polysulfoethyl A column (2.1 × 100 mm, 5 μm, 300 Å; PolyLC, Columbia, MD, USA). Peptides were eluted with a linear gradient of 0–20% solvent B (25% (v/v) acetonitrile and 500 mM ammonium formate, pH (6.8) over 50 min followed by ramping up to 100% solvent B in 5 min. The absorbance at 280 nm was monitored and a total of 16 fractions were collected. The fractions were lyophilized and resuspended in LC solvent A (0.1% formic acid in 97% water, 3% acetonitrile). A hybrid quadrupole Orbitrap (Q Exactive) MS system (Thermo Fisher Scientific, Bremen, Germany) was used with high energy collision dissociation (HCD) in each MS and MS/MS cycle as previously described [68]. It interfaced with an automated Easy-nLC 1000 system (Thermo Fisher Scientific, Bremen, Germany). Each sample fraction was loaded and carried out a Acclaim Pepmap 100 pre-column (20 mm × 75 μm; 3 μm-C18) and an PepMap RSLC analytical column (250 mm × 75 μm; 2 μm-C18) with a flow rate at 300 nl/min of solvent A (0.1% formic acid) using 25% solvent B (0.1% formic acid, 99.9% acetonitrile) for 95 min, 98% B for 100 min.

Proteomics data analysis

The MS/MS data were processed by a thorough search considering biological modifications and amino acid substitution against a non-redundant Brassica database with decoy sequences (389,401 entries) using ProteoIQ v2.7 (Premier Biosoft, Palo Alto, CA, USA) and Proteome Discoverer v1.4 (Thermo Fisher Scientific, Bremen, Germany) with SEQUEST algorithm [69] and the following parameters: peptide tolerance at 10 ppm, tandem MS tolerance at ± 0.01 Da, peptide charges of 2+ to 4+, trypsin as the enzyme, allowing one missed cleavage, iTRAQ label and methyl methanethiosulfonate (C) as fixed modifications, and oxidation (M) and phosphorylation (S, T, Y) as variable modifications. Peptide and protein were filtered using ProteoIQ 2.7 with strict peptide and protein probabilities, 0.99 and 0.95, respectively. Peptide probability is applied to filter peptide assignments obtained from MS/MS database searching results using predictable false identification error rate [70]. Protein probability is used for filtering proteins with the likelihood that the protein assignment is correct taking into account of the peptide probability for all peptides apportioned to that protein [71]. For protein quantification, only MS/MS spectra that were unique to a particular protein and where the sum of the signal-to-noise ratios for the entire peak pairs >9 were used for quantification. The accuracy of each protein ratio is given by a calculated error factor, and a p value is given to assess whether the protein is significantly differentially expressed. The error factor is calculated as the 95% confidence error which is the weighted standard deviation of the weighted average of log ratios multiplied by Student's t test. To be identified as being significantly differentially expressed, a protein should be quantified with at least three spectra (allowing generation of a p value), a p value <0.05, and a fold change >1.2 or <0.8 with at least six unique peptides in the experimental replicates (Supplementary Table 1). In addition, Single Enrichment Analysis (SEA) was performed with the list of differential proteins using agriGO (http://bioinfo.cau.edu.cn/agriGO/) to determine specifically enriched biological processes. Proteins differentially expressed were clustered by hierarchical clustering via average linkage of Pearson correlations and the k-means clustering algorithm (k=8) using CLUSTER 3.0, and the results were visualized using Java TreeView (http://www.eisenlab.org). Subcellular location of the identified proteins was predicted using five internet tools: (1) YLoc (http://abi.inf.uni-tuebingen.de/Services/YLoc/webloc.cgi), with confidence score ≥0.4; (2) LocTree3 (https://rostlab.org/services/loctree3/), with expected accuracy ≥80%; (3) ngLOC (http://genome.unmc.edu/ngLOC/index.html), with probability ≥80%; (4) TargetP (http://www.cbs. dtu.dk/services/TargetP/), with reliability class ≤3; (5) Plant-mPLoc (http://www.csbio.sjtu.edu.cn/bioinf/plant-multi/), with no threshold value in Plant-mPLoc. Only the consistent predictions from at least two tools were accepted as a confident result. For the inconsistent prediction results among the five tools, subcellular localizations of corresponding proteins were obtained from literature if available.

RESULTS

Morphological changes of *B. napus* in response to salt stress

To determine how salt stress affects *B. napus* seedlings, we monitored their morphological responses under different salt concentrations treatment (0, 50 mM, 100 mM, 200 mM and 400 mM NaCl) at seven different time points (0, 3, 5, 7, 10, 12 and 14 days) (Supplementary Figure 1). Compared with the control plants, within 7 days of treatment under 50 mM, 100 mM, 200 mM or 400 mM NaCl, the leaves of salt-treated seedlings did not exhibit any obvious phenotype differences. After 10 days of salt treatment, when the salt concentration exceeded 100 mM, plant growth began to show slight inhibition. Some fully expanded leaves appeared chlorotic after 7 days of 400 mM NaCl treatment.

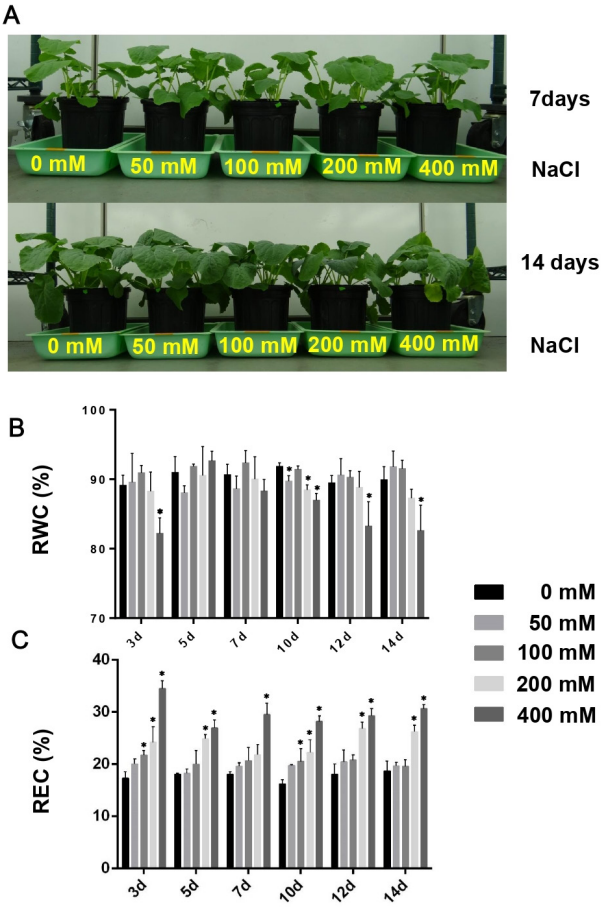

Figure 1: Morphology, relative water content (RWC) and relative electrical conductance (REC) of *B. napus* plants under salt stress for 14 days. (A) Seedlings at days 7 and 14 after 0 mM, 50 mM, 100 mM, 200 mM and 400 mM NaCl treatment. (B) RWC of leaves at 3 day, 5 day, 7 day, 10 day, 12 day and 14 day under 0 mM , 50 mM, 100 mM, 200 mM, 400 mM NaCl stress. (C) REC of leaves at 3 day, 5 day, 7 day, 10 day, 12 day and 14 day under 0 mM , 50 mM, 100 mM, 200 mM and 400 mM NaCl treatment. The values are presented as means ± standard deviation (n=3).

After 14 days of salt stress and with increasing salt concentrations from 100 mM to 400 mM, plant growth was severely inhibited (Figure 1A). Although the seedlings could survive the 14-day 400 mM NaCl treatment, they began to wilt and lose viability.

Physiological and biochemical changes of *B. napus* in response to salt stress

The relative water contents (RWC) in leaves of *B. napus* seedlings were significantly lower in 200 mM and 400 mM NaCl treated plants than control plants from the 10th day to the 14th day of stress (Figure 1B). There was no significant difference between control and the 50 mM or 100 mM NaCl treated plants. The relative electrical conductivity (REC) in the leaves was significantly higher than control from the 3rd day of high concentration salt stress, indicating cell membrane damage by the salt stress (Figure 1C).

The overall photosynthetic efficiency including stomatal conductance (Cond), intercellular CO_2 concentration (Ci), transpiration rate (Tr), photosynthetic rate (Pn), and the chlorophyll fluorescence parameters (Fv/Fm and Fv/Fo) decreased significantly at the 5th day of 200 mM and 400 mM salt stress treatment compared to the control samples (Figure 2A-2D, 2G, 2H). Interestingly, water use efficiency (WUE) was obviously increased after the 5th day of salt stress (Figure 2E). Although the respiration rate did not decrease in the beginning of the salt treatment, it showed remarkable decreases from the 10th and 12th day of 200 mM and 400 mM salt stress (Figure 2F).

The activities of ROS scavenging enzymes, such as SOD and APX increased in response to the 200 mM and 400 mM NaCl from the 7th to 14th day (Figure 3A, 3B), while the CAT activity decreased in response to the 200 mM and 400 mM salt stress at the 10th and 14th day (Figure 3C). The GST activities did not have apparent differences except an increase at the 7th day of 400 mM NaCl treatment compared to the control samples (Figure 3D). As to the biochemical responses, *B. napus* seedlings showed accumulation of stress metabolites such as betaine, proline and soluble sugar. Betaine levels increased at the 5th day after stress and showed drastic accumulation from the 7th to 14th day under the 200 mM and 400 mM NaCl (Figure 3E). Proline levels showed obvious

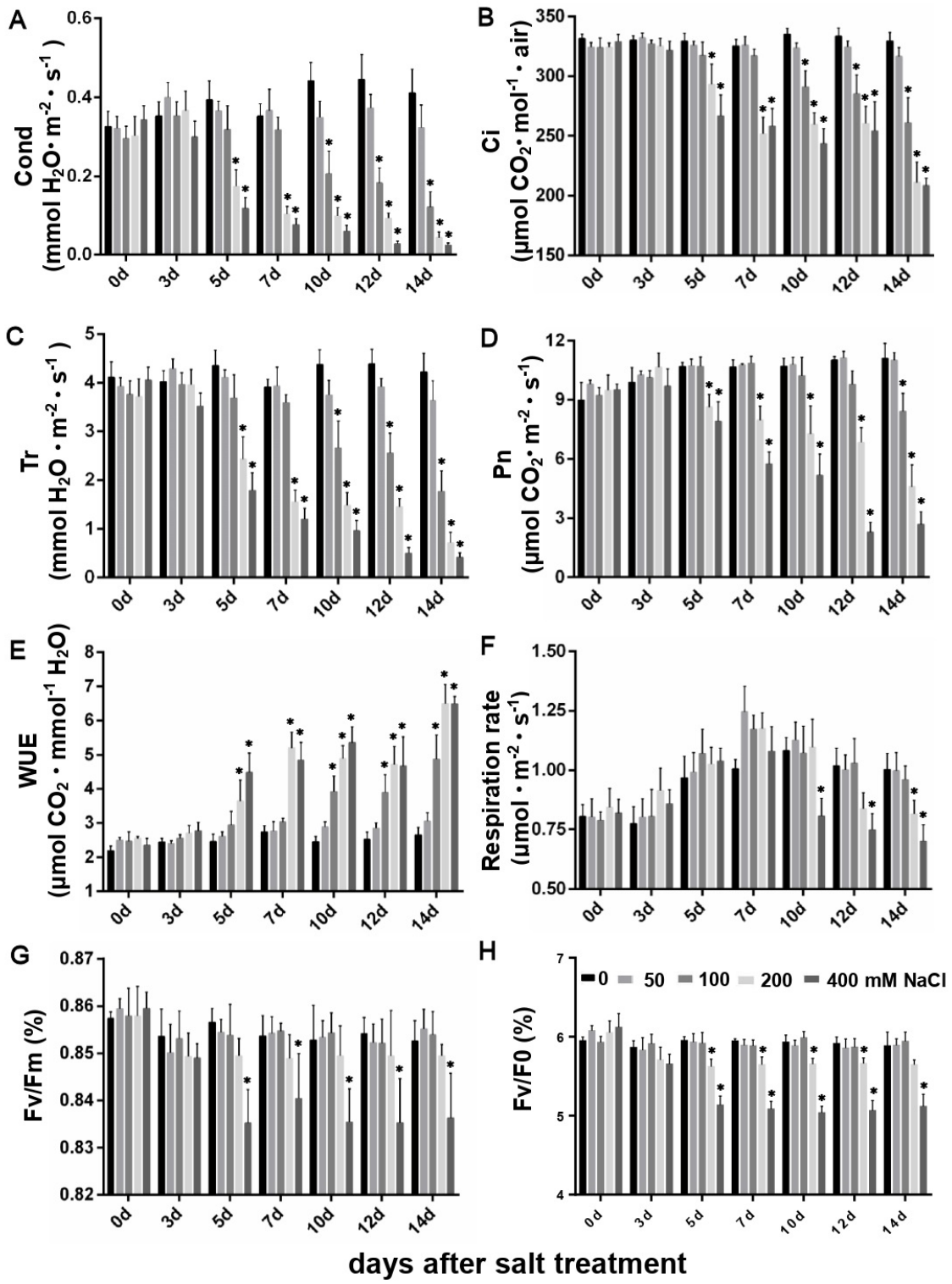

Figure 2: Temporal photosynthesis and chlorophyll fluorescence analyses of *B. napus* plants under salt stress conditions. (A) Stomatal conductance (Cond); (B) Intercellular CO_2 concentration (Ci); (C) Transpiration rate (Tr); (D) Photosynthesis rate (Pn); (E) Water usage efficiency (WUE); (F) Respiration rate; (G) Chlorophyll fluorescence parameter (Fv/Fm); (H) Chlorophyll fluorescence parameter (Fv/Fo). The data were collected at day 0, day 3, day 5, day 7, day 10, day 12 and day 14 under 0 mM , 50 mM, 100 mM, 200 mM and 400 mM NaCl conditions. The values are presented as means ± standard deviation (n=3).

increases from the 3rd day, and showed drastic accumulation from the 5th to 14th day (Figure 3F). In contrast, the soluble sugar

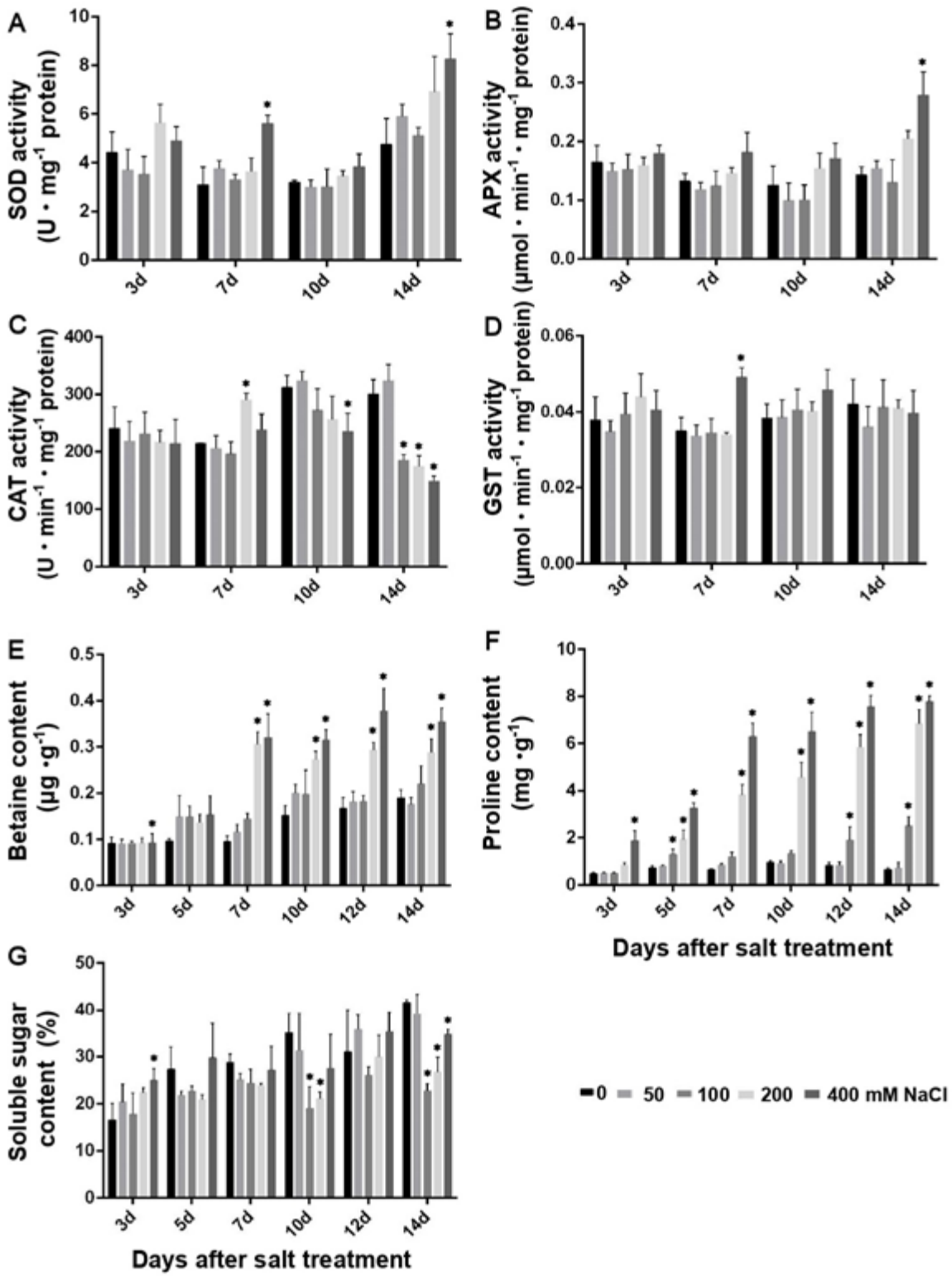

Figure 3: Antioxidant enzyme activity assay and contents of soluble sugar, proline and betaine in *B. napus* plants under salt stress. Superoxide dismutase (SOD) activity (B) Ascorbate peroxidase (APX) activity; (C) Catalase (CAT) activity; (D) Glutathione S-Transferase (GST) activity; (E) Betaine content; (F) Proline content; (G) Soluble sugar content. The data were collected at day 3, day 5, day 7, day 10, day 12 (for only E to G) and day 14 under 0 mM , 50 mM, 100 mM, 200 mM and 400 mM NaCl conditions. The values are presented as means ± standard deviation (n=3).

level did not show remarkable differences after 200 and 400 mM salt stress (Figure 3G).

Identification of differentially expressed proteins in response to salt stress

The changing trends from physiological and biological analyses were not completely the same in the course of treatments with different concentrations of salt. For example, 50 mM NaCl treatment had no effect on *B. napus* seedlings within 14 days, while after 7 days of salt treatment, the seedlings began to be affected by salt stress, and after 14 days of salt treatment they were obviously affected and inhibited by salt stress. In order to investigate the salt tolerance mechanisms, we chose three salt concentrations (100 mM, 200 mM and 400 mM NaCl) and two time points (7 day and 14 day) based on their phenotypic and physiologica responses. Using iTRAQ and 2D LC-MS/MS, a total of 2316 proteins were identified in control and salt stressed samples at a 95% confidence level (Supplementary Table 1). The identified proteins covered a wide range of biological processes (Supplementary Figure 2).

Proteomic changes were examined between the control and 100 mM, 200 mM and 400 mM NaCl treated plants at the 7^{th} day and 14^{th} day of treatment. A total of 614 proteins were determined to be differentially expressed in salt stressed samples compared to control samples (a fold change>1.2 or <0.8, $p<0.05$) (Supplementary Table 2). The differential proteins were grouped into ten functional categories based on the biological processes according to the published literatures and UniProt online analysis (https://www.uniprot.org/) (Figure 4A). They are involved in metabolism (21%), stress and defense (19%), photosynthesis (16%), protein folding and degradation (11%), transport (9%), protein synthesis (8%), signal transduction and kinase (7%), cell structure (4%), transcription related (4%) and unknown (1%). Based on agriGO functional enrichment analysis of the 614 DEPs, the DEPs involved in cellular, metabolic and response to stimulus processes were enriched under salt stress (Supplementary Figure 3). Subcellular localization analysis of the 614 DEPs revealed the top four subcellular locations as chloroplast, cytoplasm, mitochondria and nucleus (Figure 4B).

Expression patterns of the 614 DEPs fell into 27 categories (Supplementary Table 3). At 7 day of salt stress, there were 77 increased and 54 decreased proteins under 100 mM NaCl treatment (Supplementary Table 4), 171 increased and 35 decreased proteins under 200 mM NaCl treatment (Supplementary Table 4), and 233 increased and 99 decreased proteins under 400 mM NaCl treatment (Supplementary Table 4). At 14 day of salt stress, there were 396 increased and 29 decreased proteins under 100 mM NaCl treatment (Supplementary Table 5), 114 increased and 19 decreased proteins under 200 mM NaCl treatment (Supplementary Table 5), and 170 increased and 14 decreased proteins under 400 mM NaCl treatment (Supplementary Table 5).

Salinity-responsive protein-protein interactions

Proteins rarely act alone, and knowledge of the protein-protein interactions (PPIs) will facilitate molecular studies on diverse biological processes and provide insight into the biological functions of proteins with unknown functions [72]. The Biological General Repository for Interaction Datasets (BioGRID: http//thebiogrid.org) is an open access archive of genetic and protein interactions that are curated for all major model organism species [73]. To discover the relationship of the 614 differentially expressed proteins in response to salt stress, PPI networks were generated using the BioGRID database. After BLASTing in TAIR database (http://www.arabidopsis.org/Blast/index.jsp), 605 homologs in *Arabidopsis* of the 614 differential proteins were analyzed, and then subjected to the molecular Interaction BioGRID database for creation of proteome-scale interaction network. Among them, 138 proteins were depicted in the BioGRID database, and illuminated in six functional modules with tightly-connected clusters in the network (Figure 5 and Supplementary Tables 2 and 6). A total of 61 proteins were connected in the red module. There are six 14-3-3 proteins in the red module, and these 14-3-3 proteins are at the core, indicating that 14-3-3 proteins interact with multiple proteins to participate in signal transduction. In addition, 49 proteins were connected in the green module with the 26S proteasome at the core, indicating that it interacts with multiple proteins for potential degradation.

DISCUSSION

Salt stress affects plants at different levels, including physiological, biochemical and molecular processes, e.g., ionic imbalance, hyperosmotic stress, oxidative damage and nutrient deficiency [21,23,74]. Here we report salt stress responses in *B. napus* seedlings using an integrated physiological, biochemical, and proteomic approach.

Increased photosynthetic proteins to compensate for the decline of photosynthetic efficiency in *B. napus* leaves under salt stress

In this study, 18 proteins associated with photosynthesis were identified, 16 of which were increased and they were oxygen-evolving enhancer protein 2 (OEE2), OEE3, oxygen-evolving complex (OEC), chlorophyll a b-binding protein (CAB) , cytochrome b6-f complex protein (Cytb6f), ferredoxin $NADP^+$ reductase (FNR), Ribulose 1,5-biphosphate carboxylase/oxygenase (RubisCO), RubisCO activase (RCA), phosphoglycerate kinase (PGK), glyceraldehyde-3-phosphate dehydrogenase (GADPH), triosephosphate isomerase (TPI), transketolase (TK), ribulose-

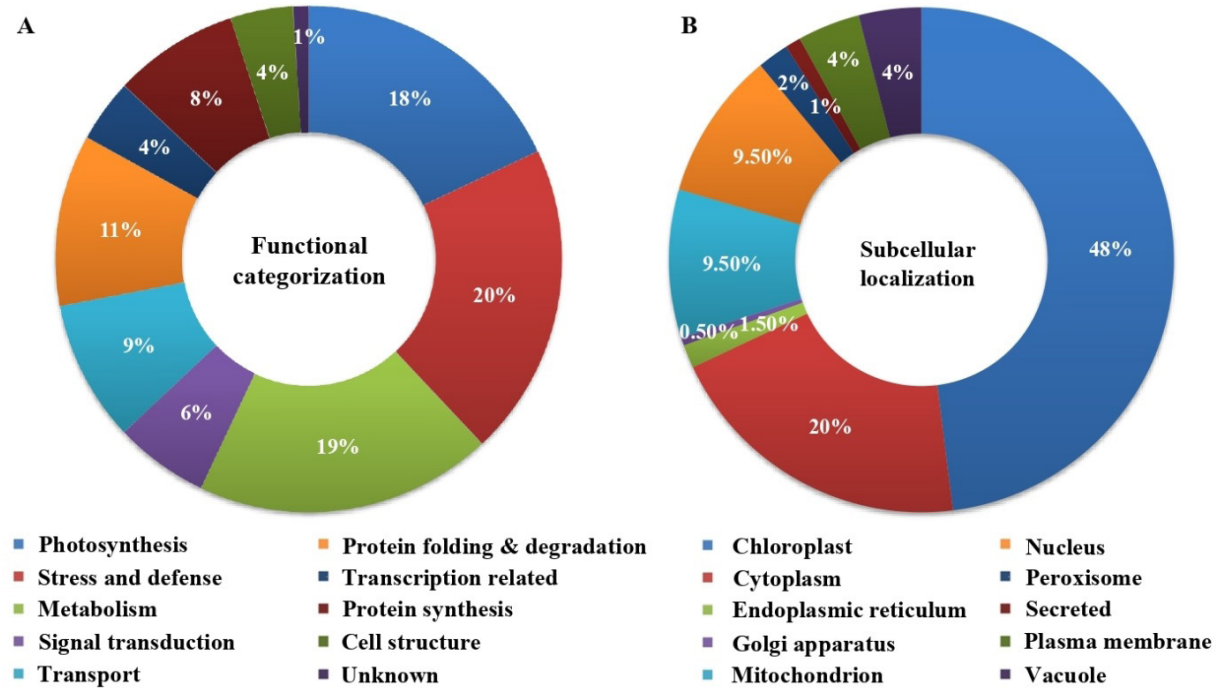

Figure 4: Functional categorization and subcellular localization of the 614 salt-stress responsive proteins in leaves of *B. napus* plants (A) The salt-stress responsive proteins were classified into 10 functional categories. The percentage of proteins in each functional category is shown in the pie (B) Subcellular localization groups of the 614 proteins. The percentage of proteins in each localization is shown in the pie.

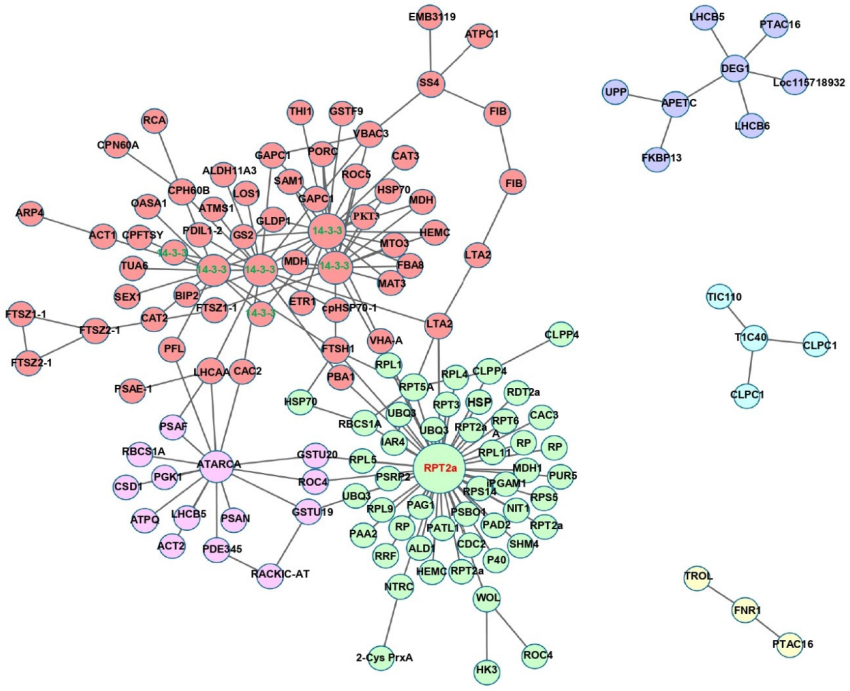

Figure 5: Protein–protein interaction (PPI) network in *B. napus* plants revealed by BioGRID analysis. A total of 138 salt responsive proteins represented from the corresponding Arabidopsis proteins are shown in PPI network. Six main groups are indicated in different colors. The PPI network is shown in the confidence view generated by BioGRID database. The abbreviations refer to Supplementary Tables 2 and 6.

5-phosphate isomerase (RPI), phosphoribulokinase precursor (PRK), magnesium-chelatase subunit chli and protochlorophyllide reductase (POR). Only a carbonic anhydrase (CA) was decreased. These proteins are involved in light reaction, Calvin cycle and chlorophyll synthesis pathways in photosynthesis. The expression levels of several proteins under salt stress are consistent with previous results. For example, OEE 2 and OEE3-1 were increased in soybean, *Vigna unguiculata* and barley under salt stress [75-77]. The CABs were also significantly increased in stress proteomics of mulberry and tea [78,79]. Cytb6f was steadily increased, and this protein was recognized as one of the salt stress-responsive markers in wheat chloroplasts [80]. The early reported increase in TK in *Arabidopsis* also agreed with the changes in TK activity observed in *Z. mays* under salt and oxidative stresses [79] and supported the hypothesis that TK was involved in plant stress protection. Proteomic studies of celery leaves revealed that magnesium chelatase (Mg chelatase) related to Chl biosynthesis showed increased abundances in cold-stress [81]. However, not all the protein changes under salt stress are consistent with previous studies. For example, a 33 kDa protein in the photosystem II oxygen-evolving complex (OEC) in white clover was decreased in abundance late in senescence, indicating degradation of photosynthetic apparatus during leaf senescence [82]. In this study, the increased OEC level showed that the photosynthetic apparatus was still stable for *B. napus* plants under salt stress for 14 days. In another proteomic study upland cotton leaves, PORs were markedly suppressed after 200 mM salt treatment for 4 h, 8 h, 24 h, 48 h and 72 h) [83,84]. Clearly, *B. napus* plants may use different mechanisms to adapt to salt stress conditions (see below).

Physiological changes of *B. napus* in response to salt stress showed the parameters related to photosynthetic efficiency (Figure 2) showed remarkable decreases compared to the control samples after the 5th day of 200 mM and 400 mM salt stress. The results are consistent with previous reports in that salt stress provoked rapid stomatal closure and impairment in CO_2 assimilation, leading to significant decreases in photosynthetic efficiency [3]. The decrease of photosynthetic efficiency may be related to cellular oxidative state under salt stress. For example, a glycolate oxidase (GO) in peroxisomes increased and can oxidize glycolate from chloroplasts to glyoxylate [85], leading intracellular H_2O_2 accumulation. Under salt stress, the activities of antioxidant enzymes (e.g., SOD and APX) increased (Figure 3). This is generally a response to increased ROS and oxidative stress [85,86]. ROS scavenging enzymes (i.e., SOD, CAT, Prx, Trx, APX, DHAR, MDHAR, GPX, GR and GST) were overrepresented in DEPs under salt stress, especially at 14 day after stress (Figure 6C). Cellular ROS scavenging system includes catalase metabolic pathway, peroxiredoxin-thioredoxin pathway (PrxR-Trx cycle) and ascorbate-glutathione cycle (AsA-GSH cycle) [86]. Under salt stress, *B. napus* cells enhanced the ROS scavenging activities to avoid oxidative damage. Nonetheless, the cells may be still under an oxidative state, as evidenced by the increased of three protein disulfide-isomerase (PDI) under salt stress (Figure 6F). PDIs are multifunctional enzymes able to facilitate oxidative folding of nascent secretory proteins in the endoplasmic reticulum (ER) [87,88]. Now how to explain the contradiction between the decreased photosynthetic efficiency and increased protein expression levels in photosynthesis in *B. napus* under salt stress? Under oxidative state, the proteins involved in photosynthesis tend to be inactive. As a positive feedback response, *B. napus* plants increased the expression of photosynthesis-related proteins (Figure 6A) as enabled by the upregulated expression of translational machinery (e.g., ribosomal proteins in Supplementary Table 2). This response compensates

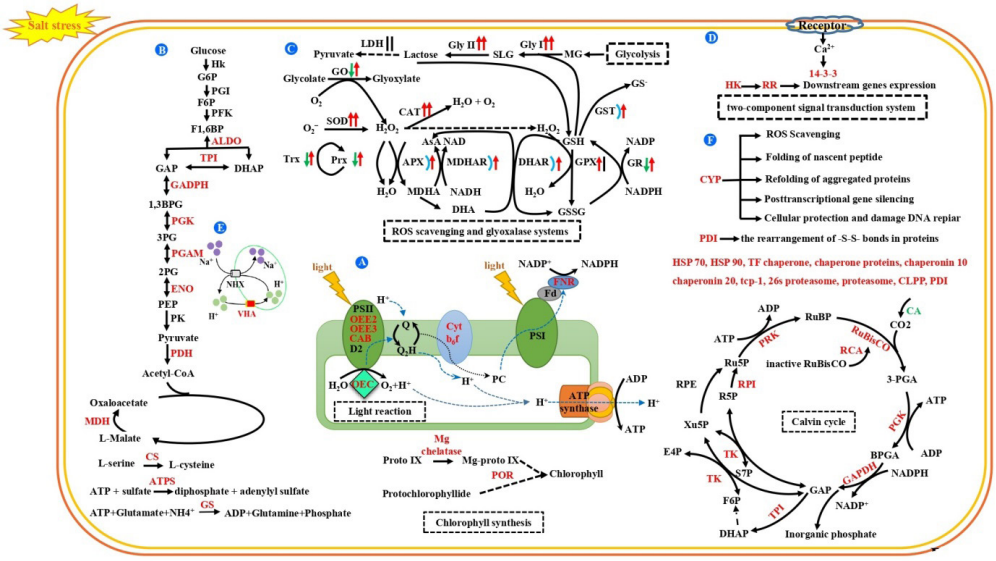

Figure 6: Schematic presentation of salt tolerance mechanisms in *B. napus* plants (A) Proteins in photosynthesis pathway. The proteins were integrated into light reaction, chlorophyll synthesis and Calvin cycle; (B) Proteins in glycolysis and the citric acid cycle; (C) Proteins involved in ROS scavenging and glyoxalase systems. The two arrows from left to right indicate days 7 and 14, respectively, with red and green showing increased and decreased, respectively. The blue arc and black lines indicate salt-stress responsive proteins and unresponsive proteins, respectively; (D) Proteins involved in signal transduction and kinases; (E) Proteins involved in iron transport; (F) Proteins involved in protein folding and degradation. Protein expression patterns under salt stress were shown by marking the proteins and reactions in red for increased proteins and in dark green for decreased proteins. Please refer to text and Supplementary Tables 2 and 7 for abbreviations.

for the decrease of photosynthetic efficiency in *B. napus*, allowing the plants to maintain photosynthesis and acquire tolerance under salt stress.

Detoxification of methylglyoxal (MG) by the glyoxalase system in *B. napus*

Under salt stress, the decreased stomatal conductance, leaf intercellular CO_2 levels and CA levels (Figure 2A, 2B and 6A), together with oxidative stress caused the decrease of photosynthesis [89]. Therefore, less oxygen was released from light reaction and the respiration rate was decreased, resulting in anaerobic respiration for limited energy production. In spite of significant increases of key enzymes involved in glycolysis (Figure 6B), the citric acid cycle of aerobic respiration was not functional. Under salt stress, glycolysis pathway could produce a highly reactive dicarbonyl metabolite, methylglyoxal (MG), through degradation of triose phosphates, glyceraldehyde-3-phosphate, and dihydroxyacetone phosphate [90]. MG has a dual role in plant cells, as a cytotoxin at high concentration or a signal molecule at low concentration [91,92]. Thus, MG homeostasis in plant cells is critical. When MG levels increase under different abiotic stresses, the glyoxalase system plays an important role in the detoxification of MG. The glyoxalase system (the glyoxalase pathway) is composed of two enzymes glyoxalase I (*Gly I*) and glyoxalase II (*Gly II*). *Gly I* detoxifies MG to S-lactoylglutathione (SLG) by using one molecule of reduced glutathione (GSH) [91,93]. Subsequently, SLG is converted to lactose by *Gly II* and one molecule of GSH is recycled back into the system [91]. In this study, five glyoxalases I (*Gly I*) and one glyoxalase II (*Gly I*) were increased in salt stressed *B. napus* plants for 7 and 14 days (Figure 6C).

In consistent with our results, overexpression of *Gly I* or *Gly II* genes in rice, *Carrizo citrange*, tomato and sugar beet plants conferred transgenic plants tolerance to salt stress and other abiotic stresses [94-97]. Transgenic plants were able to survive the various abiotic stresses through maintaining cellular MG and GSH homeostasis. Recently, the expression patterns of 16 *BrGLY I* and 15 *BrGLY II* genes from Chinese cabbage (*B. rapa*) were analyzed in different tissues and their responses to biotic and abiotic stresses. A number of BrGLY genes appeared highly responsive to these stress treatments, including salt stress, *Plasmodiophora brassicae* infection and heavy metal stress [98].

Increased signal transduction and ion transport activities to enhance salt tolerance

In plants, 14-3-3 proteins are a family of highly conserved proteins that not only regulate a variety of biological functions including signal transduction, but also interact with proteins phosphorylated on Ser or Thr residues in a conserved binding motif [99-101]. In this study, nine 14-3-3 and 14-3-3-like proteins were all increased under salt stress for 7 and 14 days (Figure 6D). Only one 14-3-3-like protein was decreased under 400 mM NaCl for 7 days. In salinity-responsive protein-protein interactions, there are six 14-3-3 proteins at the core in the red module (Figure 5). In general, the 14-3-3 interaction can change target protein localization, conformation, stability, activity, or affinity to other proteins [102,103]. 14-3-3 proteins have been reported to function in biotic and abiotic stress responses, such as salt stress [104,105]. For example, ectopic expression of a 14-3-3 adaptor gene *TaGF14b* from wheat enhanced drought and salt tolerance in transgenic tobacco [106]. *TaGF14b* expression led to enhanced ROS scavenging to ameliorate oxidative damage. In addition, a 14-3-3 gene in *Brachypodium distachyon*, *BdGF14d*, conferred salt tolerance in transgenic tobacco plants through regulating ABA signaling, ROS-scavenging, and ion transport [107].

Consistent with our results, proteomics of leaves of two upland cotton genotypes differing in salt tolerance showed that a 14-3-3-like protein E was induced by salt stress [84]. Proteomics and phosphoproteomics of sugar beet monosomic addition line M14 under salt stress showed that although the 14-3-3 protein levels did not change between salt stress and control samples, its phosphorylation modification changed under 200 mM NaCl [108]. Four 14-3-3 proteins in soybean leaves and three 14-3-3 proteins in soybean roots were dramatically increased at transcriptional and translational levels [109]. Salt-Overly-Sensitive (SOS)2-LIKE PROTEIN KINASE5 (PKS5) negatively regulates the SOS signaling pathway in *Arabidopsis* [110]. Under normal growth conditions, PKS5 phosphorylates $SOS2^{Ser294}$ and represses SOS2 activity. Upon salt stress, 14-3-3 proteins decode a salt-induced calcium signal, repress PKS5, and release SOS2 to activate H^+-ATPase and SOS1(Na^+/H^+ antiporter), thus increasing Na^+ efflux [110]. This mechanism may work similarly in *B. napus* salt-tolerance.

In addition to 14-3-3 proteins, four histidine kinases (HK) and three two-component system response and regulator (RR) were increased under salt stress (Figure 6D). Two component systems are found in bacteria, archaea, fungi, slime molds, and plants [111-113]. The receptor HK autophosphorylates on a conserved histidine residue in response to salt stress, and the phosphate is then transferred to a conserved aspartic acid residue within the receiver domain of RR proteins [114]. RR proteins frequently function as transcription factors, and phosphorylation modulates their regulation of gene expression [114]. The two-component signaling system has an established role in mediating cytokinin and ethylene signal transduction in plants [114,115]. Here the two-component signal transduction system may play an important role in transmitting salt stress signals, regulating the expression of downstream salt responsive genes to initiate salt stress response and tolerance.

In this study, six V-type H^+-ATPase (*VHA*) and five Plasma membrane ATPase (PMA) were all increased (Figure 6E). PMA, *VHA* and pyrophosphatase (PPase) are major proton pumps, providing energy for ion transport across plasma membrane and tonoplast, respectively [116,117]. Under high salt conditions, plants use an electrochemical H^+-gradient generated by the H^+ pumps to activate secondary transport of Na^+ from the cytosol into the vacuole or to extracellular space [118,119]. When

Arabidopsis VHA-c1 and c3 subunit isoforms were knocked down by RNAi, each resulted in reduced root length and decreased salt stress tolerance [120]. This result is consistent with the salt stress induced expression of *VHA* genes and *VHA* proteins in mature sugar beet leaves [121]. Ectopic expression of a wheat *VHA* gene in *Arabidopsis* and an *Arabidopsis VHA* gene in barley both improved salt tolerance of transgenic plants [122,123]. Therefore, the induced H^+ pumps in *B. napus* plants under salt stress helped to decrease cytosolic Na^+ levels, eliminate Na^+ toxicity and enhance salt resistance.

Increased proteins involved in protein folding and degradation under salt stress

Many proteins involved in protein folding and degradation were increased in *B. napus* plants under salt stress, including 12 heat shock proteins (HSPs), 12 chaperone/chaperonin proteins, 9 peptidyl-prolyl cis-trans isomerase cyclophilins chaperone proteins (CYP), 10 proteasome proteins, and 3 protein disulfide-isomerase (PDI) (Figure 6F). Consistent with our results, HSP70 expression was enhanced in salt-treated sugarcane [124], and in salt-stress tolerant potato plants [125]. Overexpression of HSP70 in *A. thaliana* led to decreased membrane damage and remarkable tolerance to heat, drought and salinity compared to the wild type control plants [124-128]. These studies concluded that HSP70 is crucial to alleviate the damage of membrane peroxidation, especially in chloroplasts, and thus confers salt tolerance.

CYPs are ubiquitous proteins found in bacteria, fungi, insects, plants and mammals. Most of them, if not all, have peptidyl-prolyl cis-trans isomerase (PPIase) activities [129]. CYP expression has been shown to be induced by biotic and abiotic stresses [130-133]. A hypothetical model depicting possible mechanisms through which cyclophilins exert their stress protective properties (Figure 6F) includes ROS Scavenging, folding of nascent proteins, refolding of aggregated proteins, posttranscriptional gene silencing, cellular protection and DNA repair [129]. Proteasomes constitute one of the main cellular proteolytic mechanisms. They recognize and degrade peptides and proteins to maintain the equilibrium between normal protein production and degradation, or to eliminate the damaged, misfolded/unfolded or pathogenic proteins [134]. The most important protease increased during the proteotoxic stress is the 26S proteasome [135,136]. This ATP-dependent proteolytic machinery works in tandem with ubiquitin to direct the selective breakdown of aberrant proteins and short-lived proteins [137]. Such capabilities are important for plant salt-stress tolerance.

Other metabolic and stress and defense proteins important for salt stress tolerance

Five cysteine synthases (CS) were all increased salt stress for 7 and 14 days (Figure 6B). CSs are key enzymes for synthesizing L-cysteine from L-serine. In consistent with our result, another proteomic study of salt stress responsive proteins in roots and leaves of rice showed that a CS was increased under salt stress [138]. In addition, a CS gene from *Polygonum sibiricum Laxm* (*PcCSase1*) was transformed into yeast cells. The survival rate of the transgenic yeast was higher than the control under 10% $NaHCO_3$ and 5 M NaCl stress. The results proved that *PcCSase1* confers high salt tolerance in yeast cells by increasing the contents of cysteine and glutathione [139].

Three ATP sulfurylases (ATPS) were increased under salt stress for 7 and 14 days (Figure 6B). The ATPS mediates selenate (Se) reduction, and promotes Se and sulfur (S) uptake and assimilation. The roles of nitric oxide (NO) and sulfur (S) on stomatal responses and photosynthetic performance were studied in mustard (*B. juncea* L) under salt stress [140]. These plants receiving NO plus S exhibited increased activities of ATPS and antioxidant enzymes, minimizing oxidative stress. Four glutamine synthetases (GS) were also increased in salt stressed *B. napus* plants (Figure 6B). The GSs are involved in nitrogen metabolism via ammonium assimilation which catalyzes the ATP-dependent biosynthesis of glutamine from glutamate and ammonia [141]. Consistent with our results, the salt tolerance of *A. thaliana* and *Z. mays* was enhanced by inoculation with Bacillus amyloliquefaciens SQR9, which produces spermidine. Spermidine was shown to increase GS gene expression, leading to increased levels of GSH, which is critical for ROS scavenging [104].

CONCLUSION

Through morphological, physiological and biochemical analyses, together with high-coverage iTRAQ-based quantitative proteomics, we conducted a comprehensive temporal study of *B. napus* salt-stress response and tolerance under different salt-stress conditions. A total of 614 DEPs were identified to include a range of biological processes, including stress and defense, metabolism and photosynthesis. As shown in Figure 6, the salt tolerance strategies of *B. napus* mainly include: (1) Increased levels of proteins associated with photosynthesis is a feedback mechanism to compensate for the decline of photosynthetic efficiency under salt stress; (2) Anaerobic respiration caused by stomatal closure and decreased photosynthesis led to cytotoxic MG production. Enhanced activities of the glyoxalase system and antioxidant systems can facilitate MG detoxification and ROS scavenging, respectively, for cellular redox homeostasis; (3) Increased 14-3-3 proteins, HKs and two-component system RR proteins ensure efficient stress signal transduction and activation of proton pumps for ion balance; (4) Increased HSPs, CYPs, proteasomes and PDIs involved in protein folding and degradation under salt stress are important salt-stress adaptive responses. This study revealed interesting salt tolerance mechanisms in *B. napus*, which lay the foundation for functional studies and potential applications in molecular breeding of stress-tolerance crops.

SUPPLEMENTARY MATERIAL

Refer to Web version on PubMed Central for supplementary material.

SUPPORTING INFORMATION

Appendix S1. A PDF file of Supplementary Figure 1 to 3 and

Supplementary Table 3, 6 and 7.

Appendix S2. Excel files of Supplementary Table 1, 2, 4 and 5.

DATA AVAILABILITY STATEMENT

The proteomics data generated in this study have been submitted to Massive repository (MSV000084676) and can be accessed via username ybgirl, password 123456789 and proteomeXchange# PXD016710.

ACKNOWLEDGEMENT

This research was supported by the National Science Foundation of China (Grant No. 31671751 and 31801426), the Natural Science Foundation of Heilongjiang Province (Grant No. C2017057), the Common College Science and Technology Innovation Team of Heilongjiang Province (Grant No. 2014TD004) and China Postdoctoral Science Foundation (204968).

REFERENCES

1. Mostek A, Börner A, Badowiec A, Weidner S. Alterations in root proteome of salt-sensitive and tolerant barley lines under salt stress conditions. J Plant Physiol. 2015;174:166-176.
2. Wu H, Ye H, Yao R, Zhang T, Xiong L. Osjaz9 acts as a transcriptional regulator in jasmonate signaling and modulates salt stress tolerance in rice. Plant Sci. 2015;232:1-12.
3. Chaves MM, Flexas J, Pinheiro C. Photosynthesis under drought and salt stress: Regulation mechanisms from whole plant to cell. Ann Bot. 2008;103:551-560.
4. Hasegawa PM. Sodium (Na^+) homeostasis and salt tolerance of plants. Environ Exp Bot. 2013;92:19-31.
5. Munns R, Tester M. Mechanisms of salinity tolerance. Annu Rev Plant Biol. 2008;59:651-681.
6. Sleimi N, Guerfali S, Bankaji I. Biochemical indicators of salt stress in plantago maritima: Implications for environmental stress assessment. Ecol Indic. 2015;48:570-577.
7. Sobhanian H, Aghaei K, Komatsu S. Changes in the plant proteome resulting from salt stress: Toward the creation of salt-tolerant crops? J Proteomics. 2011;74:1323-1337.
8. Yu J, Chen S, Zhao Q, Wang T, Yang C, Diaz C, et al. Physiological and proteomic analysis of salinity tolerance in puccinellia tenuiflora. J Proteome Res. 2011;10:3852-3870.
9. Mekawy AM, Assaha DV, Yahagi H, Tada Y, Ueda A, Saneoka H, et al. (2015) Growth, physiological adaptation, and gene expression analysis of two egyptian rice cultivars under salt stress. Plant Physiol Biochem. 2015;87:17-25.
10. Flowers TJ, Yeo AR. Breeding for salinity resistance in crop plants: Where next? Aust J Plant Physiol. 1995;22:875-884.
11. Pardo JM. Biotechnology of water and salinity stress tolerance. Curr Opin Biotechnol. 2010;21:185-196.
12. Ikbal FE, Hernández JA, Barba-Espín G2, Koussa T, Aziz A, Faize M, et al. Enhanced salt-induced antioxidative responses involve a contribution of polyamine biosynthesis in grapevine plants. J Plant Physiol. 2014;171:779-788.
13. Rishi A, Sneha S. Antioxidative defense against reactive oxygen species in plants under salt stress. Int J Curr Res. 2017;5:1622-1627.
14. Pang Q, Chen S, Dai S, Chen Y, Wang Y, Yan X, et al. Comparative proteomics of salt tolerance in Arabidopsis *thaliana* and *Thellungiella halophila*. J Proteome Res. 2010;9:2584-2599.
15. Zhu JK. Salt and drought stress signal transduction in plants. Annu Rev Plant Biol. 2002;53:247-273.
16. Nanjo T, Kobayashi M, Yoshiba Y, Sanada Y, Wada K, Tsukaya H, et al. Biological functions of proline in morphogenesis and osmotolerance revealed in antisense transgenic arabidopsis *thaliana*. Plant J. 1999;18:185-193.
17. Wang Y, Sun G, Suo B, Chen G, Wang J, Yan Y, et al. Effects of Na2CO3 and NaCl stresses on the antioxidant enzymes of chloroplasts and chlorophyll fluorescence parameters of leaves of Puccinellia tenuiflora (Turcz.) scribn et Merr. Acta Physiol Plant. 2008;30:143-150.
18. Zhao G, Han Y, Sun X, Li S, Shi Q. Salinity stress increases secondary metabolites and enzyme activity in safflower. Ind Crop Prod. 2015;64:175-181.
19. Yıldıztugay E, Sekmen AH, Turkan I, Kucukoduk M. (2011) Elucidation of physiological and biochemical mechanisms of an endemic halophyte Centaurea tuzgoluensis under salt stress. Plant Physiol Biochem. 2011;49:816-824.
20. Parvin S, Lee OR, Sathiyaraj G, Khorolragchaa A, Kim YJ, Yang DC, et al. Spermidine alleviates the growth of saline-stressed ginseng seedlings through antioxidative defense system. Gene. 2014;537:70-78.
21. Hernandez JA, Campillo A, Jimenez A, Alarcon JJ, Sevilla F. Response of antioxidant systems and leaf water relations to NaCl stress in pea plants. New Phytol. 1999;141:241-251.
22. Zhang H, Han B, Wang T, Chen S, Li H, Zhang Y, et al. (2012) Mechanisms of plant salt response: Insights from proteomics. Proteome Res. 2012;11:49-67.
23. Zhao Q, Zhang H, Wang T, Chen S, Dai S. Proteomics-based investigation of salt-responsive mechanisms in plant roots. J Proteomics. 2013;82:230-253.
24. Pandit A, Rai V, Sharma TR, Sharma PC, Singh NK. Differentially expressed genes in sensitive and tolerant rice varieties in response to salt-stress. J Plant Biochem Biot. 2011;20:149-154.
25. Fan XD, Wang JQ, Yang N, Dong YY, Liu L, Wang FW, et al. Gene expression profiling of soybean leaves and roots under salt, saline-alkali and droughtstress by high-throughput Illumina sequencing. Gene. 2013;512:392-402.
26. Jiang Y, Deyholos MK. (2006) Comprehensive transcriptional profiling of NaCl-stressed *arabidopsis* roots reveals novel classes of responsive genes. BMC Plant Biol. 2006;6:25.
27. Wang H, Miyazaki S, Kawai K, Deyholos M, Galbraith DW, Bohnert HJ, et al. Temporal progression of gene expression responses to salt shock in maize roots. Plant Mol Biol. 2003;52:873-891.

28. Long W, Zou X, Zhang X. (2015) Transcriptome analysis of canola (*Brassica napus*) under salt stress at the germination stage. Plos One. 2015;10:1-21.

29. Zahaf O, Blanchet S, de Zélicourt A, Alunni B, Plet J. Comparative transcriptomic analysis of salt adaptation in roots of contrasting *medicago truncatula* genotypes. Mol Plant. 2012;5:1068-1081.

30. Kawaura K, Mochida K, Yamazaki Y, Ogihara Y. Transcriptome analysis of salinity stress responses in common wheat using a 22k oligo-dna microarray. Funct Integr Genomics. 2006;6:132-142.

31. Walley JW, Sartor RC, Shen Z, Schmitz RJ, Wu KJ, Urich M A et al. Integration of omic networks in a developmental atlas of maize. Sci. 2016; 353:814–818.

32. Karp NA, Huber W, Sadowski PG, Charles PD, Hester SV, Lilley KS. Addressing accuracy and precision issues in iTRAQ quantitation. Mol Cell Proteomics. 2010; 9:1885–1897.

33. Kang G, Li G, Wang L, Wei L, Yang Y, Wang P, et al. Hg-responsive proteins identified in wheat seedlings using iTRAQ analysis and the role of ABA in Hg stress. J Proteome Res. 2015;14:249–267.

34. Xu J, Lan H, Fang H, Huang X, Zhang H, Huang J, et al. Quantitative proteomic analysis of the rice (*Oryza sativa* L.) salt response. Plos One. 2015;10:1-19.

35. Liu D, Ford KL, Roessner U, Natera S, Cassin AM, Pattersob HJ, et al. Rice suspension cultured cells are evaluated as a model system to study salt responsive networks in plants using a combined proteomic and metabolomic profiling approach. Proteomics. 2013;13:2046-2062.

36. Cui D, Wu D, Liu J, Li D, Xu C, Li S, et al. Proteomic analysis of seedling roots of two maize inbred lines that differ significantly in the salt stress response. Plos One. 2015;10:1–13.

37. Gong B, Zhang C, Li X, Wen D, Wang S, Shi Q, et al. Identification of NaCl and $NaHCO_3$ stress responsive proteins in tomato roots using iTRAQ-based analysis. Biochem Biophys Res Commun. 2014;446:417–422.

38. Yang L, Zhang Y, Zhu N, Koh J, Ma C, Pan Y, et al. Proteomic analysis of salt tolerance in sugar beet monosomic addition line M14. J Proteome Res. 2013;12:4931–4950.

39. Wang L, Liang W, Xing J, Tan F, Chen Y, Huang L, et al. Dynamics of chloroplast proteome in salt-stressed mangrove *Kandelia candel* (L.) Druce. J Proteome Res. 2013;12:5124–5136.

40. Cheng T, Chen J, Zhang J, Shi S, Zhou Y, Lu L, et al. Physiological and proteomic analyses of leaves from the halophyte *Tangut Nitraria* reveals diverse response pathways critical for high salinity tolerance. Front Plant Sci. 2015;6:30.

41. Shokri-Gharelo R, Noparvar PM. Molecular response of canola to salt stress:Insights on tolerance mechanisms. Peer J. 2018;6:1–22.

42. Carré P, Pouzet A. Rapeseed market, worldwide and in Europe. OCL. 2014;21:1–12.

43. Milazzo MF, Spina F, Vinci A, Espro C, Bart JCJ. Brassica biodiesels:Past, present and future. Renew Sust Energ Rev. 2013;18:350–389.

44. Yang Y, Zheng Q, Liu M, Long X, Liu Z, Shen Q, et al. Difference in sodium spatial distribution in the shoot of two canola cultivars under saline stress. Plant Cell Physiol. 2012; 53:1083–1092.

45. Bybordi A, Tabatabaei J, Ahmedov A. The influence of salinity stress on antioxidant activity in canola cultivars (*Brassica napus* L.). J Food Agric Environ. 2010;8:122–127.

46. Ashraf M, Ali Q. Relative membrane permeability and activities of some antioxidant enzymes as the key determinants of salt tolerance in canola (*Brassica napus* L.). Environ Exp Bot. 2008;63:266–273.

47. Sakr MT, El-Sarkassy NM, Fuller MP. Osmoregulators proline and glycine betaine counteract salinity stress in canola. Agron Sustain Dev. 2012;32:747–754.

48. Heidari M. Nucleic acid metabolism, proline concentration and antioxidants enzyme activity in canola (Brassica nupus L.) under salinity stress. Agr Sci China. 2010;9:504–511.

49. Akbari GA, Hojati M, Modarres-Sanavy SAM, Ghanati F. Exogenously applied hexaconazole ameliorates salinity stress by inducing an antioxidant defense system in *Brassica napus* L. plants. Pestic Biochem Phys. 2011;100:244–250.

50. Bandehagh A, Salekdeh GH, Toorchi M, Mohammadi A, Komatsu S. Comparative proteomic analysis of canola leaves under salinity stress. Proteomics. 2011;11:1965–1975.

51. Jia H, Shao M, He Y, Guan R, Chu P,Jiang H. Proteome dynamics and physiological responses to short-term salt stress in *Brassica napus* leaves. PLoS One. 2015;10:e0144808.

52. Yıldız M, Akçalı N, Terzi H. Proteomic and biochemical of canola responses (*Brassica napus* L.) exposed to salinity stress and exogenous lipoic acid. J Plant Physiol.2015;179:90–99.

53. Chandramouli K, Qian PY. Proteomics: Challenges, techniques and possibilities to overcome biological sample complexity. Hum Genomics and Proteomics 2009:204–239.

54. Lan P, Li W, Wen TN, Shiau JY, Wu YC, Lin W, et al. iTRAQ protein profile analysis of *Arabidopsis* roots reveals new aspects critical for iron homeostasis. Plant Physiol. 2011;155:821–834.

55. Owiti J, Grossmann J, Gehrig P, Dessimoz C, Laloi C, et al. iTRAQ-based analysis of changes in the cassava root proteome reveals pathways associated with post-harvest physiological deterioration. Plant J. 2011;67:145–156.

56. Banaei-Asl F, Farajzadeh D, Bandehagh A, Komatsu S. Comprehensive proteomic analysis of canola leaf inoculated with a plant growth-promoting bacterium, *Pseudomonas fluorescens*, under salt stress. Biochim Biophys Acta. 2016;1864:1222–1236.

57. Koh J, Chen G, Yoo MJ, Zhu N, Dufresne D, Erickson EJ, et al. Comparative proteomic analysis of *Brassica napus* in response to drought stress. J Protteome Res. 2015;14:3068–3081.

58. Smart RE, Bingham GE. Rapid Estimates of Relative Water Content. Plant Physiol. 1974;53:258–260.

59. Dionisio-Sese ML, Tobita S. Antioxidant responses of rice seedlings to salinity stress. Plant Sci. 1998;135:1–9.

60. Willits DH, Peet MM. Measurement of chlorophyll fluorescence as a heat stress indicator in tomato: Laboratory and greenhouse comparisons. J Am Soc Horti Sci. 2001;126:188–194.

61. Stewart RRC, Bewley JD. Lipid peroxidation associated with accelerated aging of soybean axes. Plant Physiol. 1980;65:245–248.

62. Nakano Y, Asada K. Hydrogen peroxide is scavenged by ascorbate-specific peroxidase in spinach chloroplasts. Plant Cell Physiol. 1980;22:867–880.

63. Davis DG, Swanson HR. Activity of stress-related enzymes in the perennial weed leafy spurge (Euphorbia esula L.). Environ Exp Bot. 2001;46:95–108.

64. Abei H. Catalase in vitro. Methods Enzymol. 1984;105:121–126.

65. Li HS, Sun Q, Zhao SJ, Zhang WH. Principles and techniques of plant physiological biochemical experiment. Higher Education Press:Beijing. 2000.

66. Grieve CM, Maas EV. Betaine accumulation in salt: Tressed sorghum. Physiol Plantarum. 2006;61:167–171.

67. Koh J, Chen S, Zhu N, Yu F, Soltis PS, Soltis ED. Comparative proteomics of the recently and recurrently formed natural allopolyploid tragopogon mirus (asteraceae) and its parents. New Phytol. 2012;196:292–305.

68. Makarov A, Denisov E, Kholomeev A, Balschun W, Lange O , Struoat K, et al. Performance evaluation of a hybrid linear ion trap/orbitrap mass spectrometer. Anal Chem. 2006;78:2113–2120.

69. Eng JK, McCormack AL, Yates JR. An approach to correlate tandem mass spectral data of peptides with amino acid sequences in a protein database. J Am Soc Mass Spectrom. 1994;5:976–989.

70. Keller A, Nesvizhskii AI, Kolker E, Aebersold R. Empirical statistical model to estimate the accuracy of peptide identifications made by MS/MS and database search. Anal Chem. 2002;74:5383–5392.

71. Nesvizhskii AI, Keller A, Kolker E, Aebersold R. A statistical model for identifying proteins by tandem mass spectrometry. Anal Chem. 2003;75:4646-4658.

72. Wiles AM, Doderer M, Ruan J, Gu TT, Ravi D, Blackman B, et al. (2010) Building and analyzing protein interactome networks by cross-species comparisons. BMC Syst Biol. 2010;4:36.

73. Chatr-Aryamontri A, Oughtred R, Boucher L, Rust J, Chang C, Kolas NK, et al. The BioGRID interaction database:2017 update. Nucleic Acids Res. 2017;45:D369-D379.

74. Xiong L, Zhu JK. Abiotic stress signal transduction in plants: Molecular and genetic perspectives. Physiol Plant. 2001;112:152-166.

75. Ma H, Song L, Shu Y, Wang S, Niu J, Wang Z, et al. Comparative proteomic analysis of seedling leaves of different salt tolerant soybean genotypes. J Proteomics. 2012;75:1529-1546.

76. De Abreu CE, Araújo Gdos S, Monteiro-Moreira AC, Costa JH, Leite Hde B, Batista Moreno FBM, et al. Proteomic analysis of salt stress and recovery in leaves of *Vigna unguiculata* cultivars differing in salt tolerance. Plant Cell Rep. 2014;33:1289-1306.

77. Wu D, Shen Q, Qiu L, Han Y, Ye L, Jabeen Z, et al. Identification of proteins associated with ion homeostasis and salt tolerance in barley. Proteomics. 2014;14:1381-1392.

78. Guha A, Sengupta D, Reddy AR. Polyphasic chlorophyll a fluorescence kinetics and leaf protein analyses to track dynamics of photosynthetic performance in mulberry during progressive drought. J Photochem Photobiol B. 2013;119:71-83.

79. Wang Y, Fan K, Wang J, Ding ZT, Wang H, BI CH, et al. Proteomic analysis of Camellia sinensis (L.) reveals a synergistic network in the response to drought stress and recovery. J Plant Physiol. 2017;219:91-99.

80. Kamal AH, Cho K, Kim DE, Uozumi N, Chung KY, Lee SY, et al. Changes in physiology and protein abundance in salt-stressed wheat chloroplasts. Mol Biol Rep. 2012;39:9059-9074.

81. Huang W, Ma HY, Huang Y, Li Y, Wang GL, et al. Comparative proteomic analysis provides novel insights into chlorophyll biosynthesis in celeryunder temperature stress. Physiol Plant. 2017;161:468-485.

82. Wilson KA, McManus MT, Gordon ME, Jordan TW. The proteomics of senescence in leaves of white clover, Trifolium repens (L.). Proteomics. 2002;2:1114-1122.

83. Ashraf M. (2002) Salt tolerance of cotton: Some new advances. CRC Crit Rev Plant Sci. 2002;21:1-30.

84. Gong W, Xu F, Sun J, Peng Z, He S, Pan Z, et al. iTRAQ-based comparative proteomic analysis of seedling leaves of two upland cotton genotypes differing in salt tolerance. Front Plant Sci. 2017;8:2113.

85. Rojas C, Mysore KS. (2012) Glycolate oxidase is an alternative source for H_2O_2 production during plant defense responsesand functions independently from NADPH oxidase. Plant Signal Behav. 2012;7:752-755.

86. Rivero RM, Shulaev V, Blumwald E. Cytokinin-dependent photorespiration and protection the of photosynthesis during water deficit. Plant Physiol. 2009;150:1530-1540.

87. Kersteen EA, Barrows SR, Raines RT. Catalysis of protein disulfide bond isomerization in a homogeneous substrate. Biochemistry. 2011;44:12168-12178.

88. Sevier CS, Kaiser CA. Formation and transfer of disulphide bonds in living cells. Nat Rev Mol Cell Biol. 2002;3:836-847.

89. Yi X, Hargett SR, Frankel LK, Bricker TM. The PsbQ protein is required in *Arabidopsis* for photosystem II assembly/stability and photoautotrophy under low light conditions. J Biol Chem. 2006;281:26260-26267.

90. Rabbani N, Thornalley PJ. Methylglyoxal, glyoxalase 1 and the dicarbonyl proteome. Amino Acids. 2012;42:1133-1142. [PubMed:20963454]

91. Li Z. Methylglyoxal and glyoxalase system in plants: Old players, new concepts. Bot Rev. 2016;82:183-203.

92. Kaur C, Singla-Pareek SL, Sopory SK. (2014) Glyoxalase and methylglyoxal as biomarkers for plant stress tolerance. Crit Rev Plant Sci. 2014;33:429-456.

93. Mostofa MG, Ghosh A, Li ZG, Siddiqui MN, Fujita M, Tran LSP, et al. Methylglyoxal-a signaling molecule in plant abiotic stress responses. Free Radic Biol Med. 2018;22:96-109.

94. Zeng Z, Xiong F, Yu X, Gong X, Luo J, Jiang Y, et al. Overexpression of a glyoxene, OsGly I, improves abiotic stress tolerance and grain yieldin rice (*Oryza sativa* L.). Plant Physiol Biochem. 2016;109:62-71.

95. Alvarez-Gerding X, Cortés-Bullemore R, Medina C, Romero-Romero JL, Inostroza-Blancheteau C, Aquea F, et al. Improved salinity tolerance in *carrizo citrange* rootstock through overexpression of glyoxalase system genes. Biomed Res Int. 2015;2015:1-7.

96. Alvarez Viveros MF, Inostroza-Blancheteau C, Timmermann T, González M, Arce-Johnson P. Overexpression of GlyI and GlyII genes in transgenic tomato (Solanum lycopersicum Mill.) plants confers salt tolerance by decreasing oxidative stress. Mol Biol Rep. 2013;40:3281-3290.

97. Wu C, Ma C, Pan Y, Gong S, Zhao C, Chen S, et al. Sugar beet M14 glyoxalase I gene can enhance plant tolerance to abiotic stresses. J Plant Res. 2013;126:415-425.

98. Yan G, Xiao X, Wang N, Zhang F, Gao G, Xu K, Chen B, et al. Genome-wide analysis and expression profiles of glyoxalase gene families in Chinese cabbage (Brassica rapa L.). PLoS One. 2018;13:e0191159.

99. Cao H, Xu Y, Yuan L, Bian Y, Wang L, Zhen S, et al. Molecular characterization of the 14-3-3 gene family in *Brachypodium distachyon* L. reveals high evolutionary conservation and diverse responses to abiotic stresses. Front Plant Sci. 2016;7:1099.

100. Van Kleeff PJ, Jaspert N, Li KW, Rauch S, Oecking C, de Boer AH, et al. Higher order *Arabidopsis* 14-3-3 mutants show 14-3-3 involvement in primary root growth both under control and abiotic stress conditions. J Exp Bot. 2014;65:5877-5888.

101. Yashvardhini N, Bhattacharya S, Chaudhuri S, Sengupta DN. Molecular characterization of the 14-3-3 gene family in rice and its expression studies under abiotic stress. Planta. 2018;247:229-253.

102. Paul AL, Denison FC, Schultz ER, Zupanska AK, Ferl RJ. 14-3-3 phosphoprotein interaction networks-does isoform diversity present functional interaction specification? Front Plant Sci. 2012;3:190.

103. Tan T, Cai J, Zhan E, Yang Y, Zhao J, Guo Y, et al. (2016) Stability and localization of 14-3-3 proteins are involved in salt tolerance in *Arabidopsis*. Plant Mol Biol. 2016;93400.

104. Chen L, Liu Y, Wu G, Zhang N, Shen Q, Zhang R, et al. Beneficial rhizobacterium bacillus amyloliquefaciens SQR9 induces plant salt tolerance through spermidine production. Mol Plant Microbe Interact. 2017;30:423-432.

105. Liu Q, Zhang S, Liu B. (2016) 14-3-3 proteins: Macro-regulators with great potential for improving abiotic stress tolerance in plants. Biochem Biophys Res Commun. 2016;477:9-13.

106. Zhang Y, Zhao H, Zhou S, He Y, Luo Q, Zhang F, et al. Expression of *TaGF14b*, a 14-3-3 adaptor protein gene from wheat, enhances drought and salt tolerance in transgenic tobacco. Planta. 2018;248:117-137.

107. He Y, Zhang Y, Chen L, Wu C, Luo Q. A member of the 14-3-3 gene family in *Brachypodium distachyon*, *BdGF14d*, confers salt tolerance in transgenic tobacco plants. Front Plant Sci. 2017;8:340.

108. Yu B, Li J, Koh J, Dufresne C, Yang N, Qi S, et al. Quantitative proteomics and phosphoproteomics of sugar beet monosomic addition line M14 in response to salt stress. J Proteomics. 2016;143:286-297.

109. Ji W, Cong R, Li S, Li R, Qin Z, Li Y, et al. Comparative proteomic analysis of soybean leaves and roots by iTRAQ provides insights into response mechanisms to short-term salt stress. Front Plant Sci. 2016;7:573.

110. Yang Z, Wang C, Xue Y, Liu X, Chen S, Song CP, et al. Calcium-activated 14-3-3 proteins as a molecular switch in salt stress tolerance. Nat Commun. 2010;10:1199.

111. Mizuno T. Two-component phosphorelay signal transduction systems in plants: From hormone responses to circadian rhythms. Biosci Biotechnol Biochem. 2005;69:2263-2276.

112. Schaller GE, Shiu SH, Armitage JP. Two-component systems and their co-option for eukaryotic signal transduction. Curr Biol. 2011;21:R320-R330.

113. Gao R, Stock AM. Biological insights from structures of two component proteins. Annu Rev Microbiol. 2009;63:133-154.

114. Binder BM, Kim HJ, Mathews DE, Hutchison CE, Kieber JJ, Schaller GE, et al. (2018) A role for two-component signaling elements in the *Arabidopsis* growth recovery response to ethylene. Plant Direct. 2018;2:e00058.

115. Gruhn N, Heyl A. Updates on the model and the evolution of cytokinin signaling. Curr Opin Plant Biol. 2013;16:569-574.

116. Zhang XH, Li B, Hu YG, Chen L, Min DH. The wheat E subunit of V-type H^+-ATPase is involved in the plant response to osmotic stress. Int J Mol Sci. 2014;15:16196-16210.

117. Gaxiola RA, Palmgren MG, Schumacher K. Plant proton pumps. FEBS. 2007;581:2204-2214.

118. Qiu N, Chen M, Guo J, Bao H, Xiuling MA. Coordinate up-regulation of V-H^+-ATPase and vacuolar Na^+/H^+ antiporter as a response to NaCl treatment in a C-3 halophyte Suaeda salsa. Plant Sci. 2007;172:1218-1225.

119. Yang MF, Song J, Wang BS. Organ-specific responses of vacuolar H-ATPase in the shoots and roots of C halophyte Suaeda salsa to NaCl. J Integr Plant Biol. 2010;52:308-314.

120. Padmanaban S, Lin X, Perera I, Kawamura Y, Sze H. Differential expression of Vacuolar H^+-ATPase subunit c genes in tissues active in membrane trafficking and their roles in plant growth as revealed by RNAi. Plant Physiol. 2004;134:1514-1526.

121. Kirsch M, An Z, Viereck R, Löw R, Rausch T. Salt stress induces an increased expression of V-type H^+-ATPase in mature sugar beet leaves. Plant Mol Biol. 1996;32:543-547.

122. He X, Huang X, Shen Y, Huang Z. Wheat V-H^+-ATPase subunit genes significantly affect salt tolerance in *Arabidopsis thaliana*. Plos One. 2014;9:e86982.

123. Adem GD, Roy SJ, Huang Y, Chen Z, Wang F. Expressing *Arabidopsis thaliana* V-ATPase subunit C in barley (Hordeum vulgare) improves plant performance under saline condition by enabling better osmotic adjustment. Funct Plant Biol. 2017;44:1147.

124. Murad AM, Molinari HB, Magalhães BS, Franco AC, Takahashi FS, Quirino BF, et al. Physiological and proteomic analyses of Saccharum spp. grown under salt stress. Plos One. 2014;9:e98463.

125. Aghaei K, Ehsanpour AA, Komatsu S. Proteome analysis of potato under salt stress. J Proteome Res. 2008;7:4858-4868.

126. Zamboni A, Minoia L, Ferrarini A, Tornielli GB, Zago E. Molecular analysis of post-harvest withering in grape by AFLP transcriptional profiling. J Exp Bot. 2008;59:4145-4159.

127. Deytieux C, Geny L, Lapaillerie D, Claverol S, Bonneu M, Donèche B. Proteome analysis of grape skins during ripening. J Exp Bot. 2007;58:1851-1862.

128. Song A, Zhu X, Chen F, Gao H, Jiang J, Chen S, et al. A chrysanthemum heat shock protein confers tolerance to abiotic stress. Int J Mol Sci. 2014;15:5063-5078.

129. Galat A. Variations of sequences and amino acid compositions of proteins that sustain their biological functions: An analysis of the cyclophilin family of proteins. Arch Biochem Biophys. 1999;371:149-162.

130. Godoy AV, Lazzaro AS, Claudia AC, Segundo BS. Expression of a Solanum tuberosum cyclophilin gene is regulated by fungal infection and abiotic stress conditions. Plant Sci. 2000;152:123-134.

131. Luan S, Albers MW, Schreiber SL. Light-regulated, tissue-specific immunophilins in a higher plant. Proc Natl Acad Sci U S A. 1994;91:984-988.

132. Chou IT, Gasser CS. Characterization of the cyclophilin gene family of *Arabidopsis thaliana* and phyloge¬netic analysis of known cyclophilin proteins. Plant Mol Biol. 1997;35:873-892.

133. Sharma AD, Singh P. Effect of water stress on expression of a 20 kD cyclophilin-like protein in drought susceptible and tolerant cultivars of Sorghum. J Plant Biochem Biot. 2003;12:77-80.

134. Lefaki M, Papaevgeniou N, Chondrogianni N. Redox regulation of proteasome function. Redox Biol. 2017;13:452-458.

135. Amm I, Sommer T, Wolf DH. Protein quality control and elimination of protein waste: The role of the ubiquitin–proteasome system. Biochim Biophys Acta. 2014;1843:182-196.

136. Hanssum A, Zhong Z, Rousseau A, Krzyzosiak A, Sigurdardottir A. An inducible chaperone adapts proteasome assembly to stress. Mol Cell. 2014;55:566-577.

137. Glickman MH. Getting in and out of the proteasome. Semin Cell Dev Biol. 2000;11:149-158.

138. Liu CW, Chang TS, Hsu YK, Wang AZ, Yen HC. Comparative proteomic analysis of early salt stress responsive proteins in roots and leaves of rice. Proteomics. 2014;14:1759-1775.

139. Liu MK, Liu GJ, Wei ZG, Yan XF, Qu CP. Cloning and expression of cysteine synthase gene from *Polygonum sibiricum Laxm*. Hereditas. 2008;30:1363-1371.

140. Fatma M, Masood A, Per TS, Khan NA. Nitric oxide alleviates salt stress inhibited photosynthetic performance by interacting with sulfur assimilation in mustard. Front Plant Sci. 2016;7:521.

141. Tullius MV, Harth G, Horwitz MA. Glutamine synthetase GlnA1 is essential for growth of Mycobacterium tuberculosis in humanTHP-1 macrophages and guinea pigs. Infect Immun. 2003;71:3927-3936.